

SIMULATION OF HOM WAKEFIELDS IN THE MAIN LINACS OF ILC

R.M. Jones and C.J. Glasman, Cockcroft Institute of Accelerator Science and Technology, Daresbury, Cheshire WA4 4AD, UK and University of Manchester, Manchester M13 9PL, UK

Abstract

We investigate the electromagnetic field (e.m.) excited by a train of multiple bunches in the main superconducting linacs of the ILC. These e.m. fields are represented as a wake-field. Detailed simulations are made for the modes which constitute the long-range wake-field in new high gradient cavities. In particular, we focus our study on the modes in re-entrant cavities. Modes trapped within a limited number of cells can give rise to a significant diminution in the emittance of the beam and we pay particular attention to these modes.

INTRODUCTION

Up until 2004 there were two main technologies under consideration for an international linear collider (ILC) for electron-positron collisions; one of which was based on room temperature X-band technology known as the NLC/GLC [1, 2] and another on superconducting L-band technology known as TESLA [3]. The latter technology was adopted for the ILC by an international committee, ITRP [4] and the main superconducting cavities therein forms the focus of this paper. However, we note that there is parallel research still ongoing on a compact linear collider known as CLIC [5] which has recently adopted X-band technology. The overall footprint of the entire CLIC machine is approximately 50 km and it aims at a 3 TeV center of mass (CM) energy at the collision point, with an accelerating gradient in the main cavities of 100 MV/m.

In the ILC scenario, the nominal design now considers 2670 positron and electron bunches accelerated up to a centre of mass (CM) energy of 500 GeV at a design luminosity of $2 \times 10^{34} \text{ cm}^{-2} \text{ s}^{-1}$ [6]. Here, we confine ourselves to a discussion of the heart of the system, the main L-band linacs which in the first stage perform the function of accelerating an injected beam from 15 GeV to 500 GeV and in the projected upgrade to 1 TeV (achieved by increasing the length of each linac by an additional 11 km/per linac and increasing the overall footprint of the machine to more than 50 km). Each of these linacs contains approximately 8,000 superconducting RF (SCRF) cavities, each cavity of which is composed of nine cells. The present baseline design relies on TESLA-style cavities [2] and aims at a peak gradient of 35MV/m. The cavities are enclosed in cryomodules and in a given SCRF cryomodule there will be up to 9 cavities. To date only ten SCRF cryomodules have been fabricated [6] and it will clearly be a challenge to this meet this desired gradient with acceptable yields for the ILC.

Nonetheless, there is a significant international effort engaged on alternative designs, aiming to achieve gradients in excess of 50 MV/m, in order to reduce the

overall footprint of the collider. Two main alternative cavity designs have been focused on: a re-entrant design which is being undertaken at Cornell University and a design at KEK based on a low-loss cavity shape known as the ‘‘Ichiro’’ cavity [7]. In both designs, increasing the accelerating gradient leads to a concurrent increase in the maximum magnetic field on the walls of the cavity and this results in a quenching of the superconducting state of the Nb [8]. Re-shaping the cells of the cavities allows the ratio of the peak magnetic field to the accelerating gradient to be reduced compared to that of the baseline TESLA shape.

We focus one of the re-entrant cavity designs in which the ratio of the peak magnetic field to the accelerating field is reduced by 10 % compared to that of the TESLA cell ($H_{pk}/E_{acc} = 3.78 \text{ mT/MV}$ which in practice corresponds to a critical field of $\sim 185 \text{ mT}$ [7]) but with a 20 % increase in the peak electric field ($E_{pk}/E_{acc} = 2.40$). However, the enhanced field emission that occurs with the increase in the peak surface electric field is not thought to be a cause for concern as surface treatment techniques such as high pressure rinsing have been shown to cope with surface gradients as high as 70-80 MV/m with little field emission. This design maintains the same iris radius as the TESLA design, *viz.*, 35 mm. Thus, the short-range wake, will not change appreciably, and hence the cavity-to-cavity alignment tolerances, which depend on the transverse wake-field, will also be largely unchanged.

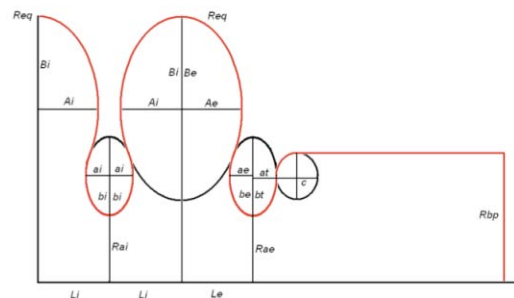


Figure 1: Reconfigured re-entrant cavity [9]

Nonetheless, the new design will repartition the bands of the higher order modes (HOMs) [10] excited by the transit of the beam through the cavities and thus the long-range wake field will differ from that in the TESLA cavities. This may well change the beam dynamics and in the worst-case give rise to trapped modes which can seriously disrupt the luminosity of the colliding beams. We have already considered a preliminary design for the cavities [11]. Here, we analyse the HOMs in a similar re-entrant cavity, which differs only in that the end cells are

modified and the beam-pipes increased in radius to 50 mm and this is illustrated in Fig. 1.

This paper is organized in the following manner. The next section discusses the eigenmodes of the transverse deflecting HOMs in a complete 9-cell cavity. The penultimate main section provides a discussion of the wake-field associated with these modes and the impact on the beam dynamics is analysed by considering the RMS of the sum of the wake-field experienced by the bunch train.

CAVITY EIGENMODES

We utilize the eigenmode solver of GdfidL [12], a code based a finite difference algorithm, to compute the electromagnetic field within a 3-D cavity structure. In our simulations each mesh line is, on average separated from its neighbour by 1 mm and this results in more than 18 million mesh cells for the complete re-entrant accelerator cavity. Additional mesh points were specified at the metallic boundaries. In order accomplish this simulation it was necessary to use a parallel version of GdfidL in which we used up to 24 nodes.

We evaluated the eigemodes and calculated the phase advance from the Floquet field relation [11]. These results are displayed in the Brillouin diagram in Fig 2. The points correspond to the discrete modes and the curves correspond to a single cell subjected to infinitely periodic boundary conditions. The infinite periodic curves are required to pass through the points

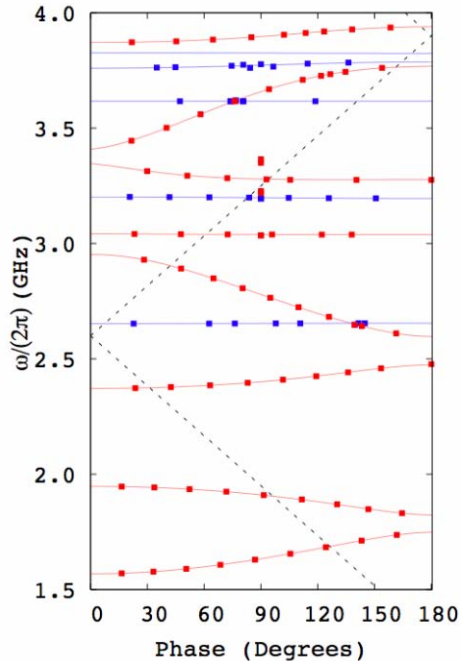


Figure 2: Brillouin diagram of re-entrant cavity for dipole (red) and sextupole (blue) modes.

representing the discrete modes. It is notable there are points in which this is not the case and these correspond to beam pipe modes of the structure, rather than cavity modes. Furthermore, the first three dipole bands are

contained below 2.5 GHz, the cut-off of a beam-pipe of radius 35 mm (the previous design). However, as the

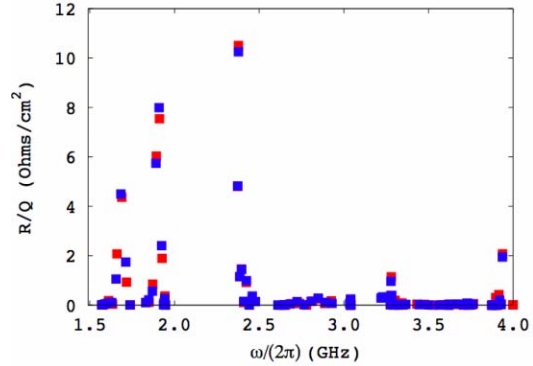


Figure 3: Cavity dipole R/Qs for the two reentrant cavity designs. Red points show the original 35mm design. Blue the redesigned expanded beam pipe geometry.

beam-pipes in this design are 50 mm beam-pipe, the cut-off is 1.76 GHz, and thus modes with frequencies above this value are able to readily propagate out of the beam-pipes This information is particularly important if we consider the kick factors [13] of each of these modes. We computed 76 R/Q values for more than 8 bands of the cavity and these are displayed in Fig 3. For a particular mode m , the kick factor is obtained from R_m/Q_m as: $K_m = cR_m/4Q_m$. It is clear that a limited number of modes dominate array of R/Q values. We retain 12 of the largest R/Q values and present them in the Table 1. At

Frequency (GHz)	R/Q (Ω/cm^2)
1.655	1.06
1.684	4.5
1.712	1.95
1.891	5.74
1.909	7.99
2.373	4.83
2.378	10.25
2.386	1.15
2.396	1.45
2.425	0.99
3.278	0.97
3.936	2.41

Table 1: R/Q of cavity dipole modes

2.378 GHz there is a mode with an R/Q of 10.25 Ω/cm^2 and as this lies below the cut-off of the beam tubes it will be able to propagate out to these regions and be properly damped. Indeed, all modes in the third dipole band are above the cut-off of the beam tubes and thus they can propagate out through the beam tubes.

In the next section we calculate the wake-field corresponding to these eigenmodes. Prior to performing these calculations we note that particularly damaging modes will be those which are trapped in the vicinity of a

limited number of cells. These modes may not have large kick factors, but they will have large Q values and have the potential to significantly dilute the emittance of the beam. In our investigations of this cavity we have discovered such candidates for trapped modes and an example of a mode, in the fourth band is illustrated in Fig. 4. This does not have a particularly large kick factor.

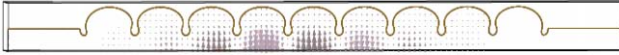


Figure 4: GdfidL simulation electric field for a trapped dipole eigenmode at 3.039GHz

We compute the wake-field from a summation of the modes [11] given in Table 1 in the next section.

TRANSVERSE WAKEFIELDS

The maximum excursion in the amplitude of the wake-field is represented by the envelope of wake-field and this is displayed in Fig. 5 for the case of a uniform damping Q of 10^5 for all modes. Clearly by 5 km the damping is

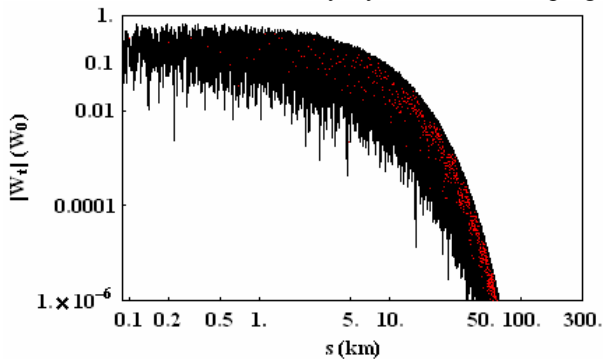


Figure 5: Envelope of transverse wakefield, normalised with respect to $W(0)$ ($= 0.16$ V/pC/mm/m).

making an impact on the diminution of the wake-field. For the nominal parameter set [6] this means 45 bunches should be adequate to represent the interaction in a particle tracking beam dynamics simulation. The onset

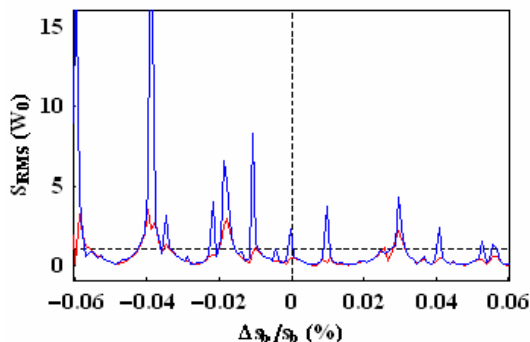


Figure 6: RMS of the sum wakefield as a function of the percentage deviation in bunch spacing from the design value for a Q of 10^6 (blue) and a Q of 10^5 (red).

of a beam break up instability is predicted by S_{RMS} , the RMS of the sum wake-field, and this is presented in Fig. 6 for two uniform Q values as a function of the deviation

of the bunch spacing from the nominal value (corresponding to small systematic changes in the mode frequencies). The modes are well spaced in frequency and as they are high Q modes then it is clear that there is little interaction between modes. From experience [14], values above unity correspond to regions in which significant emittance dilution may occur. There are several regions, close to the nominal bunch spacing in which S_{RMS} is larger than unity for a Q of 10^5 and a Q of 10^6 . In these regions emittance dilution is likely to occur unless further damping is targeted in specific cell regions of the cavity. For example for the first dipole band, a frequency shift of approximately 160 kHz will move the beam into the range of the first unstable resonance.

CONCLUSION

The alternate design cavities provide a means of achieving an appreciably higher gradient and will allow the overall footprint of the linac to be reduced. The modified wake-field must also be carefully damped to avoid BBU and emittance dilution. Recent designs have pushed the gradient up even further [15] and with a concomitant reduction in the aperture there will also be enhanced wake-fields which will require investigating.

ACKNOWLEDGEMENTS

We are pleased to acknowledge the support of W. Bruns, the author of the code GdfidL, on issues pertaining to parallel processing simulations of ILC cavities. We acknowledge the encouragement of H. Padamsee and are grateful to V. Shemelin for important advice on the parameters for the cavity studied in this work.

REFERENCES

- [1] T. O. Raubenheimer *et al.*, eds., SLAC-R-474,1996; N. Phinney, ed., SLAC-R-571, 2001.
- [2] KEK-Report-2003-7, <http://lcdev.kek.jp/Roadmap,2003>.
- [3] R. Brinkmann *et al.*, eds., DESY-2001-011, 2001.
- [4] ITRP Recommendation, http://www.fnal.gov/directorate/icfa/ITRP_Report_Final.pdf (2004).
- [5] <http://clic-study.web.cern.ch/CLIC-Study/>: CERN 2000-008, CERN 2003-007, CERN 2004-005.
- [6] N. Phinney, ICFA beam dynamics newsletter No 42, April 2007; ILCSC Parameters Document, http://www.fnal.gov/directorate/icfa/LC_parameters.pdf.
- [7] K. Saito *et al.*, Presented at 12th International Workshop on RF Superconductivity, July 10-15, NY., 2005.
- [8] R.L. Geng, Cornell SRF060209-01, 2005.
- [9] J. Luk *et al.*, Cornell SRF050808-07, 2005.
- [10] R.M. Jones *et al.*, SLAC-PUB-9467, 2002.
- [11] R.M. Jones and C. Glasman, Proc. Linac06, 2006.
- [12] W. Bruns, Proc. PAC97, 1997; <http://www.gdfidL.de>.
- [13] P.B. Wilson, SLAC-PUB-4547, 1989.
- [14] R.M. Jones *et al.*, SLAC-PUB-8108, 1999.
- [15] ILC Newslines, <http://www.linearcollider.org/>, March 2007.